Numerical Methods in Civil Engineering, 9-2 (2024) 01-16

Numerical Methods in Civil Engineering

Journal Homepage: https://nmce.kntu.ac.ir/

Numercial Analysis Of Steel Depassivation By The Action Of Chloride Ions In Reinforced Concrete Structures

Roberto Pettres [*], Ahiram Roquitski [**], Rafael Petronilho de Oliveira Rocha [***]

ARTICLE INFO

RESEARCH PAPER

Article history:
Received:
May 2024
Revised:
August 2024
Accepted:
November 2024

Keywords:
Depassivation of steel rei nforcement; Start of corrosion; Coating to retard corrosion; Diffusion equation for chloride; Boundary Element Method.

Abstract:

This paper presents an application of the Boundary Element Method (BEM) in engineering to simulate and numerically analyze the process of accumulation of chloride ions in a reinforced concrete structure. The study begins with a brief review of the origin of reinforced concrete and the phenomenon of depassivation of reinforcement. The geometric and mathematical model considers two types of concrete characteristics, seeking to numerically represent the concrete used in the construction of beams and pillars of buildings and bridges, covered with an external layer and/or surface protection. In the simulations, it was possible to record the concentration of chlorides in the position occupied by a steel rod in the reinforcement, calculating the number of years necessary to cause the steel to depassivate. In addition to concrete, two materials with different diffusivities were used for the coating layer and two values for its thickness, both related to the time required for the start of the reinforcement corrosion process. The results were obtained with a correlation level of 0.99954 for the R^2 estimator, presented in the formulation validation section 4.1, allowing to obtain important information about the steel depassivation process with and without the use of surface protection, making it possible to calculate the start time of reinforcement depassivation under different conditions, the details of which are presented below.

1. Introduction

In 1855, the Frenchman Joseph Louis LAMBOT introduced “reinforced cement” to the world for the first time, a name that lasted until 1920 and is currently called reinforced concrete, based on a prototype boat built with a mesh of interlaced metal rods and concrete. This prototype was taken to the Universal Exhibition in Paris, where the ornamental plant dealer, landscaper, and horticulturist, named Joseph MONIER, found the ideal material to make vases and jugs for plants [1].

For a long time, Monier produced, used, and sold a large number of reinforced concrete pots and boxes, as they presented greater resistance when compared to equivalent structures without the use of metallic reinforcement. Monier advanced in the use of the technique, building a system of moving boxes and basins in iron and cement applicable to horticulture, whose work earned him the first patent on July 16, 1867.

New applications of the technique were carried out and gave it other patents, including a patent for a system of sleepers and supports in cement and iron applicable to streets, roads and railways (3 November 1877), a patent for a system of container tanks in cement and iron, applicable to all types of industries (March 15, 1880), patent for a system of conduit tubes in cement and iron, applicable to all types of industries for conduction and plumbing, with or without pressure, of water, gas, and all other elements and liquids of different natures (24 August 1885), patents for a new system of building fixed or portable, hygienic and economical houses in cement and iron (15 April 1886) and its last patent for a system for building cement and iron gutters with single and double ligatures, for telephone and electrical wires in general (24 April 1891) [2].

The rights to Monier's patents were acquired by G. A. Wayss in 1888 (Germany), a German civil engineer and builder

[*] *Corresponding author: UFPR – Federal University of Paraná, Postgraduate Program in Numerical Methods in Engineering, Department of Mathematics, Curitiba, Paraná, Brazil, Email: pettres@ufpr.br*
[**] *UFPR – Federal University of Paraná, Department of Statistics. Curitiba, Paraná, Brazil, Email: ahiram@ufpr.br*
[***] *UFSC – Federal University of Santa Catarina, Joinville, Santa Catarina, Brazil, , Email: rafaelpetronilho@gmail.com*

https://doi.org/10.61186/NMCE.2405.1059

who co-founded the company Wayss & Freytag (founded in 1875), who quickly undertook a series of experimental studies, assisted by another engineer, Matthias Koenen.

At the time, three items were questioned in the new reinforced cement material, the first referring to the moisture in the concrete which could accelerate the corrosion of the steel rods, the second about the possible lack of adhesion between the concrete and the steel rods and the third on the difference in deformation of concrete and steel during a temperature variation.

The company Wayss & Freytag carried out tests for 20 years to eliminate these doubts, concluding that the adhesion of steel and concrete would be satisfactory, improved with the use of bars with ribs and/or reliefs, and that concrete and steel have expansion coefficients similar thermal (and contraction) conditions, leaving a broad answer to the question about the corrosion of the bars caused by the humidity of the concrete, even more so since the steel is immersed in a concrete matrix, thus promoting a false sense of protection of the reinforcement against corrosion [3].

It is currently known that the corrosion of reinforcement is caused by different types of chemical reactions resulting from the interaction of the reinforcement with the environment in which it is inserted, being accelerated when in the presence of corrosion-inducing agents. Among the corrosion agents, the chloride ion stands out, widely spread in maritime areas, and soils rich in chlorides and also present in industrial processes that use chloride-based products [4], is considered an aggressive agent to reinforced concrete, that can penetrate concrete structures through chloride absorption and diffusion mechanisms [5, 6].

One of the most important parameters that govern the phenomenon of chloride diffusion [7] is the diffusion coefficient and/or permeability coefficient, which represents the rate of penetration speed of chloride ions in a given medium. This type of diffusive process only occurs in an aqueous medium, so the presence of water in the microstructure of the concrete pores is necessary for the ionic movement to occur, which is essential for the correct assessment of the penetration of chloride ions into the concrete [8].

The penetration of chloride ions into the concrete, together with water and oxygen, begins the process of depassivation of the thin protective layer on the steel surface, generated by the presence of the base $Ca(OH)_2$ with pH = 13. When the pH of the passivation layer is below 9 [9], there is the formation of expansive ferrous compounds, corrosion itself, resulting in an increase in the volume of the original steel, causing cracking and chipping in the concrete, triggering the problem and reducing the useful life of the structure.

We understand that the microstructure of concrete and the phenomena related to the entry of chlorides are extremely random, impacting the useful life of reinforced concrete structures, however, the aim is to, in a simplified way, numerically simulate the movement of fluids in the pores of the concrete covering at using the diffusion equation to determine the time required for the degrading agents to reach the reinforcement and accumulate before the corrosion process begins.

A classic model of the corrosion process in reinforced concrete structures is that of [10] who divides this process into two stages, initiation and propagation. Initiation corresponds to the period in which chloride ions move within the concrete mass, from the surface of the structure to the end of the covering layer, reaching the reinforcement. Propagation deals with the effects of corrosion, which begins with the depassivation of the reinforcement, culminating in the loss of the steel section and cracking of the concrete. The time of the initiation stage is considerably longer than that of propagation, therefore, durability studies are generally focused on the initiation period [8].

Initial predictions of the corrosion rates of the steel present in a piece of concrete coated with a layer of paint are found in laboratory studies based on accelerated tests of exposure to chlorides [11], which, even accelerated, can require a long period and financial resources in destructive tests to obtain results that can statistically indicate when the process of depassivation and degradation of the reinforcement begins, and it is here that the present study seeks alternatives based on computer simulations.

In Brazil, the reinforced concrete production process is standardized by ABNT NBR 6118:2014 [12], which prohibits the use of additives containing chloride in reinforced or prestressed concrete structures, as well as defining project parameters, such as nominal coverage and quality of the concrete. However, the aforementioned standard does not present specific recommendations that correlate corrosion induced by chloride ions with structural durability and it is here that, again, the study is justified and seeks to estimate with greater precision the time in which depassivation of the reinforcement begins, without and with the application of some external coating.

To this end, as a way to prevent or minimize the premature deterioration of reinforced concrete structures due to chlorides, the application of an external coating to the concrete structure was designed and simulated using the chloride diffusion equation and the sub-region technique [13], acting as a protective layer and/or coating, to create a barrier between the chlorides present in the external environment and the concrete.

The computational simulations were carried out using a hybrid mathematical formulation of BEM, which we call D-BEM, using a time-independent fundamental solution [14] and a Finite Difference Method (FDM) scheme [13] to represent the dynamics of the process. Penetration of chloride ions into the coating layer material and concrete,

calculating the concentration values of chlorides that reach and accumulate on the steel surface. In this study, only the effects of the reinforcement depassivation time were considered, that is the period at which corrosion began.

Important authors cited in references [14-27] support the theoretical aspects of the method, in addition to being references for the study of chloride ion diffusion.

In this study, the validation of the proposed formulation was carried out by comparing the numerical results with the results of a simplified problem, whose analytical solution is known, in addition to also citing papers where the formulation was successfully used in the analysis of problems governed by the equation of diffusion.

The results of the simulations led to the expansion of knowledge about the beginning of the steel corrosion process, indicating the time during which the reinforcement depassivation occurs, important information for planning prevention, and maintenance measures to extend the useful life of structures of reinforced concrete.

The solution of the system of equations was based on the Gaussian elimination method and the stability of the results of the proposed formulation was verified. The results of this study, as well as the entire boundary element formulation, are presented below.

2. Geometrical and Mathematical model

2.1 Cross section of a piece of reinforced concrete with an external coating layer - Geometric model

The real model idealized in this study is a piece of a reinforced concrete column with a unit radius with an external coating layer, illustrated in Figure 1 (A), whose internal details are illustrated in Figure 1 (B).

Assuming that the top and bottom of the concrete section are sealed with resin, preventing the flow of chloride through these faces [11] and that the chloride concentration occurs superficially over the coating layer, the numerical model can be approximated by a cross-section (two-dimensional) of the reinforced concrete element, whose layers are represented using sectorally homogeneous subregions.

Thus, the geometric model adopted for this study, illustrated in Figure 2, is a circular transversal section of the set formed by the coating layer and concrete containing the metallic reinforcement Ω_1, which for simplicity are simulated as a single material Ω_2, as the objective is only to obtain the value of chloride accumulation in the position occupied by a steel rod of the metallic reinforcement.

Figure 1 (A) illustrates a piece of reinforced concrete covered by a layer of material less permeable than concrete, similar to a layer of epoxy material or ink. In (B) the interior of the concrete piece is shown, allowing detailed observation of the steel reinforcement. Thus, as an approximation of the real problem, the geometric model used is a ring Ω_1 representing an external coating layer of thickness ***L***, a disc Ω_2 representing a concrete section with metallic reinforcement in the two-dimensional domain Ω, where $\Omega = \Omega_1 + \Omega_2 = L + X$, $\Omega(x, y) = x^2 + y^2 \leq (1+L)\ m$, illustrated in Figure 3.

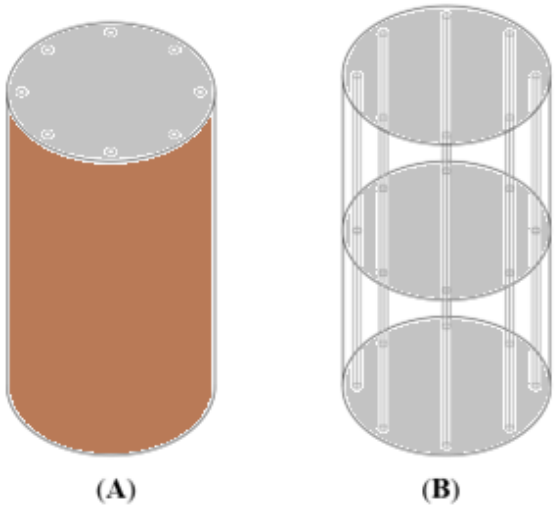

Fig. 1: A piece of reinforced concrete (A) and the interior of the piece (B).

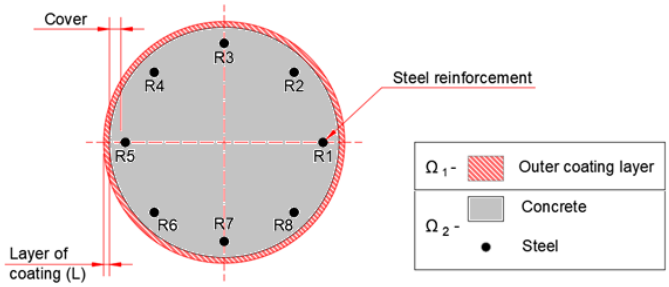

Fig. 2: Cross section of reinforced concrete piece with external coating.

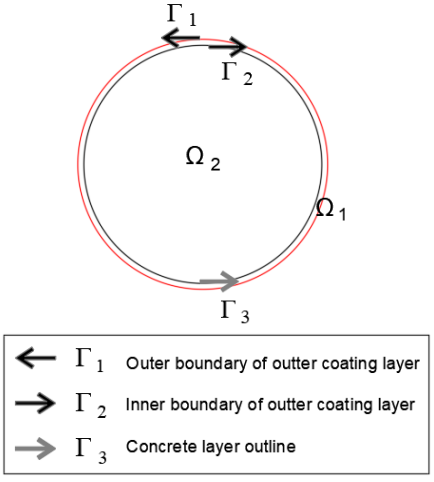

Fig. 3: Cross section of a piece of reinforced concrete with a radius equal to 1 meter.

Figure 3 illustrates the boundary elements in Γ_1 and Γ_2, with the geometry of Γ_2 coinciding with Γ_3, however, with the opposite direction due to the normal vector to the boundary of each domain, representing the contact zone between the subregions Ω_1 and Ω_2, discretized using triangular cells as shown in Figure 4, simulating the coating layer and the reinforced concrete section. It is important to note that in the contact zone, $\boldsymbol{u}$ is the same for both subregions (continuity condition) and the values of $\boldsymbol{q}$ are opposite (equilibrium condition).

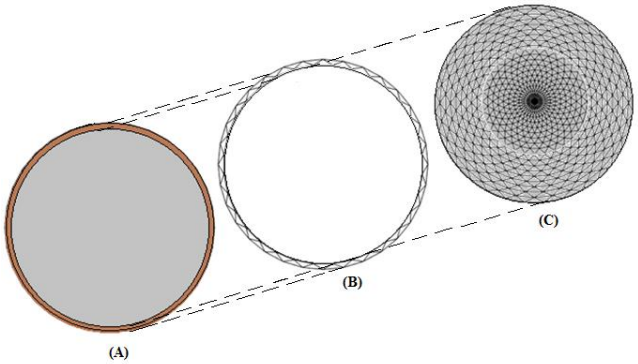

Fig. 4: Problem domain (A), a ring or sub-region indicating the cladding layer (B), and a disk or sub-region indicating the reinforced concrete section, both sub-regions discretized in triangular cells (C).

2.2 Diffusion equation with subregions - Mathematical model

Let Ω be an isotropic domain by parts, the governing diffusion equation is given by:

$$\alpha_i \nabla^2 u(X_i,t) = \frac{\partial u(X_i,t)}{\partial t} \qquad X_i \in \Omega_i,\ i=1,2 \tag{1}$$

Where α_i represents the diffusivity coefficient measured of each material measured in m^2/s, u is the concentration of chloride particles, X is the field point coordinate and t is the time variable.

Diffusion by chlorides can occur depending on the moment in which they are incorporated into the concrete [28], as suggested by Helene [29], Reis [30], and Poulsen and Mejlbro [4], in which chloride ions penetrate the concrete structure after the structure is completed, coming from the external environment, such as water, mist and sea spray, contaminated groundwater, saline solutions used for deicing, such as chloride sodium and calcium, brines from industrial processes or storage of halides or from industrial products [25]. This type of incorporation of chloride ions (Cl^-) is represented mathematically by a Dirichlet boundary condition, given by equation (2),

$$u(X,t) = Cl^-(X,t)_{environment} \qquad X \in \Gamma_1 \tag{2}$$

representing a function of the concentration of chloride ions which depends on the environment and time on the boundary over time.

The incorporation of chlorides into concrete can also occur at the time of its production, that is, in fresh concrete, where the aggregates, additives, and water used in mixing and kneading may be contaminated or contain chlorides in their composition, such as in the form of calcium chloride ($CaCl_2$) or sodium chloride (NaCl), for example. The same reasoning applies to the materials used to produce the coating. This type of incorporation of chloride ions in the concrete and in the coating layer material is represented mathematically by initial conditions, given by equations (3) and (4),

$$u(X_1,t_0) = Cl^-_{1\ \text{coating layer}} \qquad X_1 \in \Omega_1 \tag{3}$$

$$u(X_2,t_0) = Cl^-_{2\ concrete} \qquad X_2 \in \Omega_2 \qquad \Omega = \Omega_1 + \Omega_2 \tag{4}$$

representing defined amounts of chloride in the coating and concrete layer, respectively, throughout the domain only at the beginning of the simulations.

As a simplification of the real problem of chloride diffusion in concrete, the following conditions/limitations are adopted:

(i) the reinforced concrete structure is at the beginning of its useful life;
(ii) the fastest degradation agent is attacked by chlorides;
(iii) there are no accidental external factors that have affected the properties of the concrete covering;
(iv) the physical and chemical properties of concrete remain unchanged over time, highlighting the diffusivity coefficient, considered constant throughout the analysis and
(v) the effects of damage to the concrete are not considered.

The limitations imposed are intended to ensure that the mathematical formulation developed allows the analysis of the problem of depassivation of the reinforcement under the exclusive effect of chloride ions. The next section presents the formulation of boundary elements, the validation test, and the results of the tested cases.

3. D-BEM formulation

For the chloride diffusion equation, the integral equation of the D-BEM formulation can be written as follows.

$$C(\xi)u(\xi,t) = \int_\Gamma u^*(\xi,X)\,q(X,t)\,d\Gamma - \\ + \int_\Gamma q^*(\xi,X)\,u(X,t)\,d\Gamma - \frac{1}{\alpha_i}\int_\Omega \frac{\partial u(X,t)}{\partial t} u^*(\xi,X)\,d\Omega \tag{5}$$

Where $C(\xi)$ is a geometric coefficient eq.(5) at the collocation point ξ and $u*$ and $q*$ are the fundamental solution and its normal derivative, respectively.

$$C(\xi)=\begin{cases}0, \text{ if } \xi\notin\Omega\\ \frac{1}{2}, \text{ if } \xi\in\Gamma\\ 1, \text{ if } \xi\in\Omega\end{cases} \tag{6}$$

The fundamental solution $u*(\xi,X)$ used in the D-BEM formulation is independent of the time variable and is given by [31],

$$u*(\xi,X)=\frac{1}{2\pi}\ln\left(\frac{1}{r}\right) \tag{7}$$

Where $r=|X-\xi|$ is the distance between the field and collocation points.

The derivative of the fundamental solution concerning the normal direction of the boundary is given by

$$q*(\xi,X)=\frac{\partial u*}{\partial r}\frac{dr}{dn}=-\frac{1}{2\pi r}\frac{dr}{dn} \tag{8}$$

Where *n* is the outward direction normal to the boundary.

The time derivative presented in equation (5) is approximated by the backward finite difference formula [32]

$$\frac{\partial u(X,t)}{\partial t}=\frac{u(X,t+\Delta t)-u(X,t)}{\Delta t}. \tag{9}$$

Replacing equation (9) in equation (5) and grouping terms conveniently, one has the equation (10):

$$\begin{aligned}&C(\xi)u(\xi,t+\Delta t)=\int_\Gamma u*(\xi,X)\,q(X,t+\Delta t)\,d\Gamma+\\&-\int_\Gamma q*(\xi,X)\,u(X,t+\Delta t)\,d\Gamma+\\&-\frac{1}{\alpha_i\,\Delta t}\left(\int_\Omega u(X,t+\Delta t)\,u*(\xi,X)\,d\Omega-\int_\Omega u(X,t)\,u*(\xi,X)\,d\Omega\right)\end{aligned} \tag{10}$$

Equations (10) can be used recursively for the solution of diffusion problems, starting with known variables at the time t_τ and determining the unknown variables at the time $t_{\tau+1}$.

According to [30], the time step, Δt_c, can be estimated as

$$\Delta t_c \le \frac{l_j^{\,2}}{2\alpha} \tag{10}$$

Where l_j is the boundary element size.

After applying equation (10) to the boundary nodes and internal points, one obtains the following system of equations:

$$\begin{aligned}&\begin{bmatrix}\mathbf{H}_{1,1}^{bb}&\mathbf{H}_{1,2}^{bb}&0&0&0\\ \mathbf{H}_{2,1}^{bb}&\mathbf{H}_{2,2}^{bb}&0&0&0\\ \mathbf{H}_{1,1}^{db}&\mathbf{H}_{1,2}^{db}&\mathrm{I}&0&0\\ 0&0&0&\mathbf{H}_{3,3}^{bb}&0\\ 0&0&0&\mathbf{H}_{2,3}^{db}&\mathrm{I}\end{bmatrix}\begin{bmatrix}u_1^b\\u_2^b\\u_1^d\\u_3^b\\u_2^d\end{bmatrix}_{m+1}=\\&\begin{bmatrix}\mathbf{G}_{1,1}^{bb}&\mathbf{G}_{1,2}^{bb}&0\\ \mathbf{G}_{2,1}^{bb}&\mathbf{G}_{2,2}^{bb}&0\\ \mathbf{G}_{1,1}^{db}&\mathbf{G}_{1,2}^{db}&0\\ 0&0&\mathbf{G}_{3,3}^{bb}\\ 0&0&\mathbf{G}_{2,3}^{db}\end{bmatrix}\begin{bmatrix}q_1^b\\q_2^b\\q_3^b\end{bmatrix}_{m+1}+\\&-\frac{1}{\alpha_1\Delta t}\begin{bmatrix}\mathrm{M}_{1,1}^{bd}\\ \mathrm{M}_{2,1}^{bd}\\ \mathrm{M}_{1,1}^{dd}\\ \mathrm{M}_{3,2}^{bd}\\ \mathrm{M}_{2,2}^{dd}\end{bmatrix}\left\{\left[u_1^d\right]_{m+1}-\left[u_1^d\right]_m\right\}+\\&-\frac{1}{\alpha_2\Delta t}\begin{bmatrix}\mathrm{M}_{1,1}^{bd}\\ \mathrm{M}_{2,1}^{bd}\\ \mathrm{M}_{1,1}^{dd}\\ \mathrm{M}_{3,2}^{bd}\\ \mathrm{M}_{2,2}^{dd}\end{bmatrix}\left\{\left[u_2^d\right]_{m+1}-\left[u_2^d\right]_m\right\}\end{aligned} \tag{12}$$

In equation eq.(12), **H** and **G** are matrices that result from the boundary integrals related to $q*(\xi,X)u(x)$ and to $u*(\xi,X)q(x)$, respectively; the matrix **M** results from the domain integrals and I is the identity matrix. The first element of each superscript indicates the position of the source point and the second, the position of the field point, with *b* indicating boundary and *d*, domain. The subscript *m +1* indicates the time $t_{m+1}=(m+1)\Delta t$ and the subscript *m*, the time $t_m=m\Delta t$, where Δt is the time interval. In the formulation presented in this study, a constant value Δt was selected, and this value was computed according to equation (11). Similar terms in equation (12) are grouped and rewritten as equation (13):

$$\begin{aligned}&\begin{bmatrix}\mathbf{H}_{1,1}^{bb}&\mathbf{H}_{1,2}^{bb}&\frac{1}{\alpha_1\Delta t}\mathrm{M}_{1,1}^{bd}&0&0\\ \mathbf{H}_{2,1}^{bb}&\mathbf{H}_{2,2}^{bb}&\frac{1}{\alpha_1\Delta t}\mathrm{M}_{2,1}^{bd}&0&0\\ \mathbf{H}_{1,1}^{db}&\mathbf{H}_{1,2}^{db}&\mathrm{I}+\frac{1}{\alpha_1\Delta t}\mathrm{M}_{1,1}^{dd}&0&0\\ 0&0&0&\mathbf{H}_{3,3}^{bb}&\frac{1}{\alpha_2\Delta t}\mathrm{M}_{3,2}^{bd}\\ 0&0&0&\mathbf{H}_{2,3}^{db}&\mathrm{I}+\frac{1}{\alpha_2\Delta t}\mathrm{M}_2^{dd}\end{bmatrix}\begin{bmatrix}u_1^b\\u_2^b\\u_1^d\\u_3^b\\u_2^d\end{bmatrix}_{m+1}=\\&\begin{bmatrix}\mathbf{G}_{1,1}^{bb}&\mathbf{G}_{1,2}^{bb}&0\\ \mathbf{G}_{2,1}^{bb}&\mathbf{G}_{2,2}^{bb}&0\\ \mathbf{G}_{1,1}^{db}&\mathbf{G}_{1,2}^{db}&0\\ 0&0&\mathbf{G}_{3,3}^{bb}\\ 0&0&\mathbf{G}_{2,3}^{db}\end{bmatrix}\begin{bmatrix}q_1^b\\q_2^b\\q_3^b\end{bmatrix}_{m+1}+\frac{1}{\alpha_1\Delta t}\begin{bmatrix}\mathrm{M}_{1,1}^{bd}\\ \mathrm{M}_{2,1}^{bd}\\ \mathrm{M}_{1,1}^{dd}\\ \mathrm{M}_{3,2}^{bd}\\ \mathrm{M}_{2,2}^{dd}\end{bmatrix}\left[u_1^d\right]_m+\frac{1}{\alpha_2\Delta t}\begin{bmatrix}\mathrm{M}_{1,1}^{bd}\\ \mathrm{M}_{2,1}^{bd}\\ \mathrm{M}_{1,1}^{dd}\\ \mathrm{M}_{3,2}^{bd}\\ \mathrm{M}_{2,2}^{dd}\end{bmatrix}\left[u_2^d\right]_m\end{aligned} \tag{13}$$

Transferring the column coefficients of the matrices on the right-hand in equation (13) corresponding to the unknowns, to the left-hand side of the equation, one has equation (14):

$$\begin{bmatrix} \mathbf{H}_{1,1}^{bb} & \mathbf{H}_{1,2}^{bb} & \frac{1}{\alpha_1 \Delta t}\mathrm{M}_{1,1}^{bd} & 0 & 0 & -\mathbf{G}_{1,2}^{bb} & 0 \\ \mathbf{H}_{2,1}^{bb} & \mathbf{H}_{2,2}^{bb} & \frac{1}{\alpha_1 \Delta t}\mathrm{M}_{2,1}^{bd} & 0 & 0 & -\mathbf{G}_{2,2}^{bb} & 0 \\ \mathbf{H}_{1,1}^{db} & \mathbf{H}_{1,2}^{db} & \mathrm{I}+\frac{1}{\alpha_1 \Delta t}\mathrm{M}_{1,1}^{dd} & 0 & 0 & -\mathbf{G}_{1,2}^{db} & 0 \\ 0 & 0 & 0 & \mathbf{H}_{3,3}^{bb} & \frac{1}{\alpha_2 \Delta t}\mathrm{M}_{3,2}^{bd} & -\mathbf{G}_{3,3}^{bb} & 0 \\ 0 & 0 & 0 & \mathbf{H}_{2,3}^{db} & \mathrm{I}+\frac{1}{\alpha_2 \Delta t}\mathrm{M}_{2}^{dd} & -\mathbf{G}_{2,3}^{db} & 0 \end{bmatrix} \begin{bmatrix} u_1^b \\ u_2^b \\ u_1^d \\ u_3^b \\ u_2^d \\ q_2^b \\ q_3^b \end{bmatrix}_{m+1}$$

$$= \begin{bmatrix} \mathbf{G}_{1,1}^{bb} \\ \mathbf{G}_{2,1}^{bb} \\ \mathbf{G}_{1,1}^{db} \\ 0 \\ 0 \end{bmatrix} \left[q_1^b\right]_{m+1} + \frac{1}{\alpha_1 \Delta t} \begin{bmatrix} \mathrm{M}_{1,1}^{bd} \\ \mathrm{M}_{2,1}^{bd} \\ \mathrm{M}_{1,1}^{dd} \\ \mathrm{M}_{3,2}^{bd} \\ \mathrm{M}_{2,2}^{dd} \end{bmatrix} \left[u_1^d\right]_m + \frac{1}{\alpha_2 \Delta t} \begin{bmatrix} \mathrm{M}_{1,1}^{bd} \\ \mathrm{M}_{2,1}^{bd} \\ \mathrm{M}_{1,1}^{dd} \\ \mathrm{M}_{3,2}^{bd} \\ \mathrm{M}_{2,2}^{dd} \end{bmatrix} \left[u_2^d\right]_m \qquad (14)$$

Applying the equilibrium and compatibility equations in the interface between Ω_1 and Ω_2,

$$\begin{aligned} \mathbf{u}_{2,3}^b &= \mathbf{u}_3^b \\ \mathbf{q}_{2,3}^b &= -\mathbf{q}_3^b \end{aligned} \qquad (11)$$

allow reducing the number of unknowns of the system of equation (15) to the same number of equations:

$$\begin{bmatrix} \mathbf{H}_{1,1}^{bb} & \mathbf{H}_{1,2}^{bb} & \frac{1}{\alpha_1 \Delta t}\mathrm{M}_{1,1}^{bd} & \mathbf{G}_{1,2}^{bb} & 0 \\ \mathbf{H}_{2,1}^{bb} & \mathbf{H}_{2,2}^{bb} & \frac{1}{\alpha_1 \Delta t}\mathrm{M}_{2,1}^{bd} & \mathbf{G}_{2,2}^{bb} & 0 \\ \mathbf{H}_{1,1}^{db} & \mathbf{H}_{1,2}^{db} & \mathrm{I}+\frac{1}{\alpha_1 \Delta t}\mathrm{M}_{1,1}^{dd} & \mathbf{G}_{1,2}^{db} & 0 \\ 0 & \mathbf{H}_{3,3}^{bb} & 0 & -\mathbf{G}_{3,3}^{bb} & \frac{1}{\alpha_2 \Delta t}\mathrm{M}_{3,2}^{bd} \\ 0 & \mathbf{H}_{2,3}^{db} & 0 & -\mathbf{G}_{2,3}^{db} & \mathrm{I}+\frac{1}{\alpha_2 \Delta t}\mathrm{M}_{2}^{dd} \end{bmatrix} \begin{bmatrix} u_1^b \\ u_2^b = u_3^b \\ u_1^d \\ q_2^b = -q_3^b \\ u_2^d \end{bmatrix}_{m+1} =$$

$$\begin{bmatrix} \mathbf{G}_{1,1}^{bb} \\ \mathbf{G}_{2,1}^{bb} \\ \mathbf{G}_{1,1}^{db} \\ 0 \\ 0 \end{bmatrix} \left[q_1^b\right]_{m+1} + \frac{1}{\alpha_1 \Delta t} \begin{bmatrix} \mathrm{M}_{1,1}^{bd} \\ \mathrm{M}_{2,1}^{bd} \\ \mathrm{M}_{1,1}^{dd} \\ \mathrm{M}_{3,2}^{bd} \\ \mathrm{M}_{2,2}^{dd} \end{bmatrix} \left[u_1^d\right]_m + \frac{1}{\alpha_2 \Delta t} \begin{bmatrix} \mathrm{M}_{1,1}^{bd} \\ \mathrm{M}_{2,1}^{bd} \\ \mathrm{M}_{1,1}^{dd} \\ \mathrm{M}_{3,2}^{bd} \\ \mathrm{M}_{2,2}^{dd} \end{bmatrix} \left[u_2^d\right]_m \qquad (16)$$

Equation (14) can be rearranged as equation (16) and solved with the same time marching scheme used previously.

After imposing the initial and boundary conditions, the system of equations (16) is solved and the unknown potential and flux values at the boundary nodes and potential values at the internal points are determined at the time $t_{\tau+1}$. The potential values are updated and the problem solution continues, recursively.

Numerical simulations were performed on a computer with an Intel Core i5-7200U processor, 2.5 GHz with Turbo Boost up to 3.1 GHz. Results and validation of the formulation D-BEM for the chloride diffusion equation are presented below.

4. Validation and results of the D-BEM formulation

4.1 D-BEM formulation - Validation

The D-BEM formulation was implemented in Matlab R2023® software and applied to the geometric model illustrated in Figure 2, under the following boundary and initial conditions.

$$u(X_{\Gamma_1}, t) = 2 \qquad X_{\Gamma_1} \in \Gamma_1 \qquad (12)$$

Which corresponds to a constant percentage concentration of chlorides outside the coating layer, with a value equal to 2% concerning the concrete mass along the entire boundary and fixed for the entire analysis interval and

$$u(X_{1,2}, t_0) = 0 \qquad \begin{matrix} X_{1,2} \in \Omega \\ \Omega = \Omega_1 + \Omega_2 \end{matrix} \qquad (13)$$

Which corresponds to a constant and zero concentration of chlorides in the problem domain at the initial analysis time.

In this validation stage, the subregions Ω_1 and Ω_2 were considered as the same material, with diffusivity coefficient $\alpha_1 = \alpha_2 = 1\ m^2/s$, and the numerical analysis was carried out using 32 linear boundary elements and 1248 constant triangular domain cells, whose techniques for integrating boundary elements and domain cells are described in detail in [33].

The purpose of this analysis was to verify the performance of the formulation developed from BEM about the analytical result, which, in polar coordinates, is given by [33]

$$u(r,t) = \bar{u} - \frac{2\bar{u}}{R} \sum_{n=1}^{\infty} \frac{J_0(\lambda_n r)}{\lambda_n J_1(\lambda_n R)} e^{-\alpha \lambda_n^2 t} \qquad (19)$$

where R is the unit radius of the domain, and J_0 and J_1 are first kind Bessel functions of orders zero and one respectively. The parameters λ_n are the positive roots of the equation $J_0(\lambda_n) = 0$ and the first 100 roots were used.

Proceeding as indicated previously, the following results were obtained for the variation in chloride concentration $\Delta Cl^-(r,t) = u(r,t) - u(r,0)$, where r = 0.2657, 0.53173, and 0.85,coinciding with the position of the steel rod R1 (Figure 2).This practice is very important, as it avoids problems in data analysis in cases that refer to the penetration of chlorides, without considering the initial concentration of chlorides present in the concrete matrix.

To verify the significance of the values obtained numerically with the D-BEM, the statistical method of linear regression was applied to the numerical and analytical results until their convergence, and the coefficient of determination R^2 (square of the Pearson coefficient) was calculated. The value of R^2 very close to unity indicates a strong relationship between the two variables [34]. These results and the distribution of chloride variation values at the position of the steel rod R1 and r = 0.2657, 0.53173, are illustrated by the Figure 5.

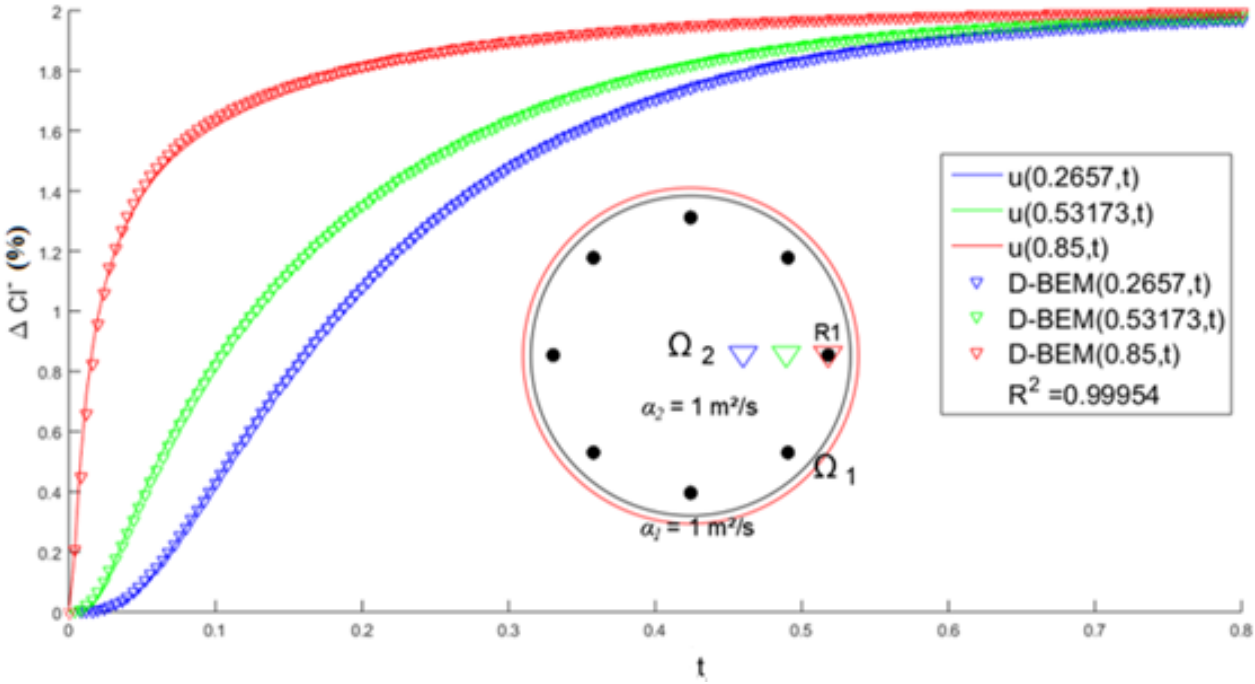

Fig. 5: Comparison between the analytical solution and D-BEM at domain points

For this simulation, R^2 was obtained equal to 0.99954, indicating excellent correlation between the variables, validating the D-BEM formulation. This D-BEM formulation was successfully used in applied diffusion problems in studies by [32, 33, 35, 36], whose results corroborate the efficiency of the formulation used. The tested cases for different coating layers and types of concrete are presented in the next section.

4.2 D-BEM formulation - Results

In the cases presented below, the concentration of chlorides is defined as a boundary condition, simulating different environments in which there is the presence of a considerable amount of chlorides, and which, through the diffusion of ions, penetrates the covering layers until reaching the reinforcement.

In the tests carried out, the results of chloride concentrations in the position of a metal reinforcement rod were compared in 4 tests. The first test simulated concrete without any coating layer, and in tests 2, 3, and 4, different materials were tested in an external coating layer. As it is a numerical experiment, the different tests were carried out using variable geometric and physical-chemical parameters, where different thicknesses and types of coating layers were also tested, as well as different types of concrete, the purpose of which is to obtain a profile of the effect of the variation of these parameters on the concentration of chlorides in the position of the steel rod and determine the moment at which corrosion begins.

It is assumed that the beginning of reinforcement corrosion occurs when the chloride concentration reaches 0.2% of the cement mass (for Portland cement concrete), this value is suggested by *Du Béton* Euro-International Committee[37] and Arora et al. [38]. The diffusivity coefficientwas calculated as a function of the water/cement ratio in the concrete using the equation obtained empirically by [39], which, according to [38], the simplifying assumption of a diffusion coefficient constant does not affect model predictions.

The analysis of the simulations will be done using two graphs, one in the form of curves relating variation in the number of chlorides over time and the other as a bar graph, indicating the time from which the depassivation of the steel begins, or beginning of corrosion, both in each of the cases studied. The time increment unit was defined in seconds, using a value corresponding to 231 days, in an analysis period of 1000 years.

4.2.1 Case 1 –Diffusion of chlorides in uncoated and coated reinforced concrete

In the first simulated case, the cross-section of the reinforced concrete piece, as shown in Figure 6, is analyzed in four

different tests presented in Table 1. In the first test (Test 1) the reinforced concrete does not present the external coating layer, as illustrated by Figure 6 (1). In the second, third, and fourth tests, three types of materials were tested for the coating layer with a thickness of 0.05 m, being the same concrete material (Test 2 - Figures 6 (2)), of a material with a diffusivity coefficientequal to 1.0 x 10^{-12} m^2/s (Test 3 - Figure 6 (3)) and 1.0 x 10^{-13} m^2/s (Test 4 - Figure 6 (4)), respectively.

The concrete was designed with Feature Compression Know, fck = 35 MPa and water/cement ratio, w/c = 0.5, resulting in a chloride diffusion coefficient equal to 5.1x10^{-11} m^2/s, a value calculated based on [40].

The numerical simulations were carried out under the following boundary and initial conditions:

$$u(X_{\Gamma_1}, t) = 2 \qquad X_{\Gamma_1} \in \Gamma_1 \tag{20}$$

which corresponds to a constant concentration of chlorides outside the coating layer along the entire contour and fixed for the entire analysis interval and

$$u(X_{1,2}, t_0) = 0 \qquad X_{1,2} \in \Omega \quad \Omega = \Omega_1 + \Omega_2 \tag{21}$$

which corresponds to a constant and zero concentration of chlorides in the problem domain at the initial analysis time.

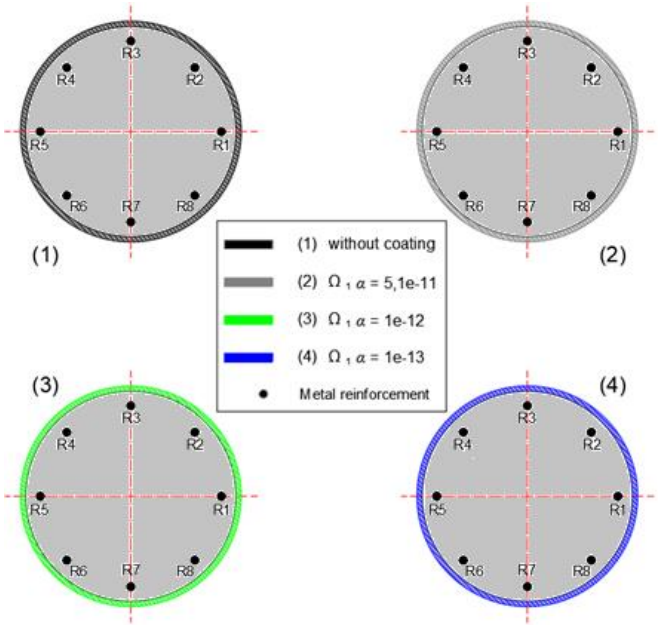

Fig. 6: Cross section of the reinforced concrete piece without and with different coatings.

Figure 7 shows the evolution of the variation in chloride concentration for the position of the steel rod R1 over 1000 years.

Table 1: Values of parameters used in simulations – Case 1.

Case 1 Test	Concrete cover (m)	Chloride diffusivity of concrete (m^2/s)	*L* = Coating thickness (m)	Chloride diffusivity of the coating (m^2/s)
1	0.05	5.1 x 10^{-11}	-	-
2	0.05	5.1 x10^{-11}	0.05	5.1 x10^{-11}
3	0.05	5.1 x10^{-11}	0.05	1.0 x 10^{-12}
4	0.05	5.1 x10^{-11}	0.05	1.0 x 10^{-13}

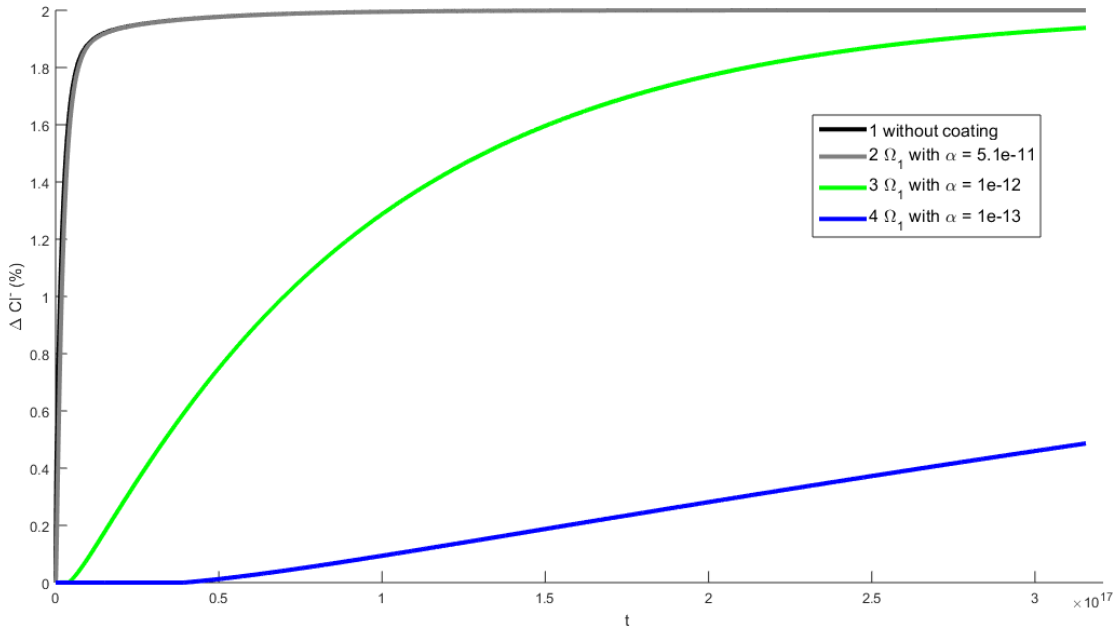

Fig. 7: Evolution of the variation in the chloride concentration of the steel rod R1 over time with a numerical error of approximately 0.0046% – Case 1. The thickness of the coating layer = 0.05 m

In Figure 7 it is possible to observe that the concentration of chlorides for tests (1 - black color) and (2 - gray color) showed similar concentration variations, converging to the value of the boundary condition, 2%, in a time interval of approximately 100 years, a period during which corrosion would possibly have deteriorated a large part of the steel rod. In the validation phase, a correlation level of 0.99956 was obtained for the R^2 estimator, indicating a numerical error of approximately 0.0046% in the amount of chlorides at the analyzed position.

Still, in Figure 7, tests (3 - green color) and (4 - blue color) show that the rate of increase in chloride concentration is slower, not reaching the value of the boundary condition in the analyzed period (1000 years).

Taking into account that the limit concentration of chlorides for the depassivation of steel is 0.2 to 0.4% [37] concerning the cement mass, it was decided to determine the time elapsed in each test until reaching the value of 0.2% of the chloride concentration.

From Figure 8 it is possible to observe that the concentration of 0.2% of chlorides in position R1 (rod 1 of the reinforcement) is reached in just less than 1 year for the unprotected concrete section, approximately 1.90 years for a coating layer of 0.05 m of the same material as concrete, 52 years for a coating layer with diffusivity coefficientequal to 1 x 10^{-12} m^2/s and just over 497 years with the use of coating with diffusivity coefficientequal to 1 x 10^{-13} m^2/s. In both cases, the times of each test show that depassivation can occur in a short period, less than 1 year, when no type of coating layer is used, however, this time can be extended if some type of external coating is applied with a material less permeable than the concrete itself.

Using the same materials defined in tests 2, 3, and 4, however, reducing the coating thickness to 0.025 m, the following chloride concentrations were obtained for the position of the steel rod R1, illustrated in Figure 9.

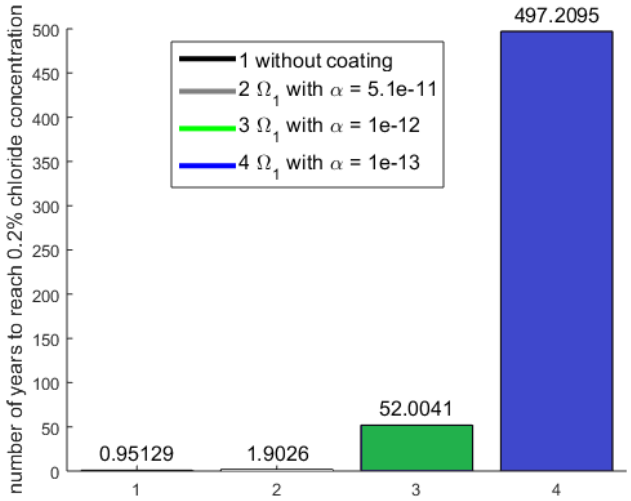

Fig. 8: Number of years to reach 0.2% of chloride concentration for different coating.The thickness of the coating layer = 0.05 m

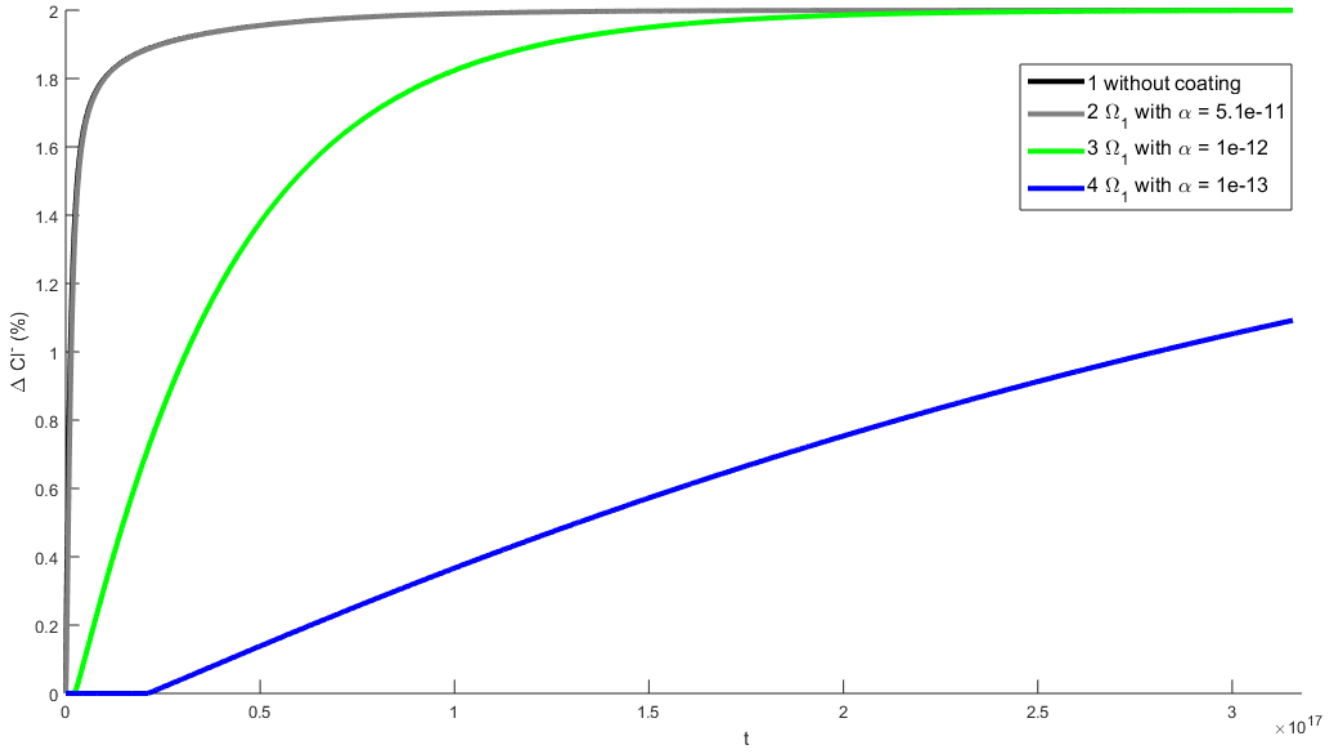

Fig. 9: Evolution of the variation in the chloride concentration of the steel rod R1 over time with a numerical error of approximately 0.0046% – Case 1. The thickness of the coating layer = 0.025 m.

Analyzing Figure 9, the evolution of the chloride concentration for the 0.025 m thick coating tests is similar to the tests carried out with a thickness of 0.05 m, however, for the test (2) the concentration variation converged to the value of the boundary condition at the beginning of the simulation period, practically coinciding with the result of test 1 without coating.

Still in Figure 9, tests (3) and (4) show that the rate of increase in chloride concentration is slower, but faster than the case with a thickness of 0.05 m, not reaching the value of the boundary condition in the analyzed period (1000 years).

Similar to the previous analysis, the time elapsed in each test until reaching 0.2% chloride concentration is illustrated in Figure 10.

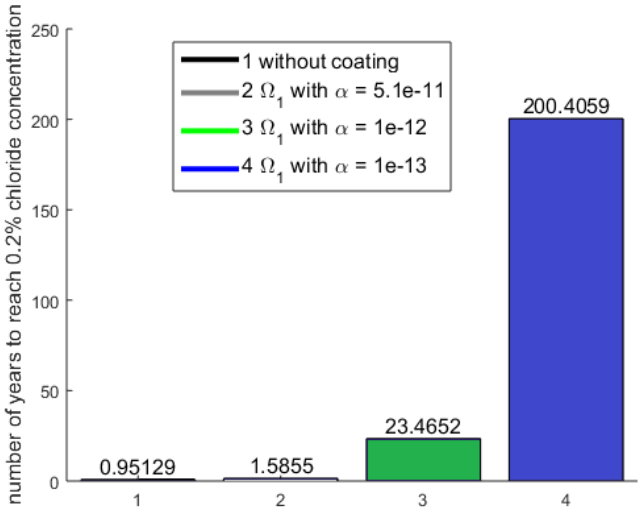

Fig. 10: Number of years to reach 0.2% of chloride concentration for different coating. The thickness of the coating layer = 0.025 m.

From Figure 10 it is possible to observe that the concentration of 0.2% of chlorides in position R1 (reinforcement rod 1) is reached after 1.58 years for a 0.025 m coating layer of the same concrete material, 23.46 years for a layer of coating with diffusivity coefficient equal to 1 x 10^{-12} m^2/s and of just over 200 years with the use of coating with diffusivity coefficient equal to 1 x 10^{-13} m^2/s. These last two results demonstrate that the use of a coating layer with a lower diffusivity coefficient than that of concrete, even with a layer of 0.025 m, can increase the time until the steel depassivation.

4.2.2 Case 2 – High-performance concrete

High-performance concrete (HPC) may be defined as concrete with strength and durability significantly beyond those obtained by conventional means. The properties required for concrete to be classified as high performance therefore depend on the concrete properties achievable at a given time and location. At present, high-performance concrete in developed countries usually refers to concrete with 28-day compressive strength beyond 70–80 MPa, durability factor (defined as the percentage of original modulus retained after 300 freeze/thaw cycles) above 80% and water/cement ratio below 0.35 [41].

According to Mehta and Monteiro [42], the most resistant HPCs are characterized by their high workability, high resistance, and low diffusivity coefficient, which means that their use is specified with a view to long durability, especially in structures subject to influences from aggressive environments.

Obtaining more resistant concrete is a significant development in the construction industry, and is present in large works such as the Petronas Twin Towers located in the city of Kuala Lumpur, Malaysia, completed in 1998 with 88 floors and 452 meters high, using the HPC with fck equal to 80 MPa. HPC was also used in the E-Tower, completed in 2003 in the Brazilian city of São Paulo with 39 floors and 148 meters high, reaching 125 MPa of resistance.

Thus, in Case 2 the reinforced concrete piece was designed with fck = 80 MPa and w/c = 0.30, which according to Wood, Wilson, and Leek [43], presents typical chloride diffusion values of between 1 x 10^{-12} m^2/s (Portland cement - mixture of fly ash with silica fume) and 1.6 x 10^{-12} m^2/s (mixture of Portland cement with fly ash).

The numerical simulations for Case 2 used the same boundary and initial conditions as Case 1, given by equations (20) and (21), respectively, and the same geometric and material configurations for the external coating, presented in Table 2.

Table 2: Values of parameters used in simulations – Case 2.

Case 2 Test	Concrete cover (m)	Chloride diffusivity of concrete (m^2/s) HPC	*L* = Coating thickness (m)	Chloride diffusivity of the coating (m^2/s)
1	0.05	1 x 10^{-12}	-	-
2	0.05	1 x 10^{-12}	0.05	1 x10^{-12}
3	0.05	1 x 10^{-12}	0.05	1 x 10^{-13}
4	0.05	1 x 10^{-12}	0.025	1 x 10^{-12}
5	0.05	1 x 10^{-12}	0.025	1 x 10^{-13}

The results for Case 2 are presented below.

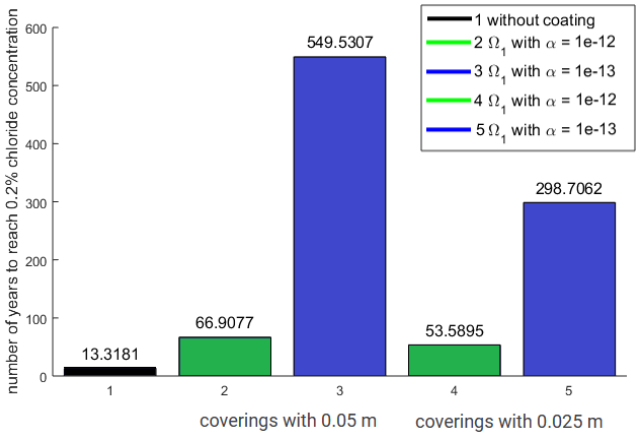

Fig. 11: Number of years to reach 0.2% of chloride concentration for different coating. Uncoated (1), thickness of the coating layer = 0.05 m (2) and (3), 0.025 m (4) and (5).

In a similar way to the analysis applied in Case 1, Figure 11 presents the values referring to the number of years for the chloride concentration to reach 0.2% in the position of the metal rod R1 using the HPC. In Test 1, without external coating, approximately 13.32 years are required, in Tests 2 and 3, using a 0.05 m coating layer, the time required was 66.90 and 549.53 years, and with a thinner layer, 0.025 m, Tests 4 and 5 indicated 53.58 and 298.70 years for the start of steel depassivation.

Comparing the results of Case 1 with Case 2, there is a significant increase in the time in which the reinforcement will not suffer deterioration due to corrosion, demonstrating that HPC can increase the useful life of a reinforced concrete structure.

This behavior was already expected since the w/c ratio directly influences the diffusivity of chlorides in concrete. In practical terms, this means that increasing the w/c ratio reduces the compactness of the concrete and increases its porosity, facilitating the diffusion of chloride ions to the reinforcement.

On the other hand, the decrease in the w/c ratio can contribute to a significant increase in the corrosion initiation time in a long-term analysis, as illustrated in Case 2. According to Cascudo[6, 44, 45], all aspects of concrete technology that contribute to obtaining a product with greater compactness (such as reducing the water/cement ratio), containing porosity that minimizes the transport of ions, gases, and liquids through its internal structure, are relevant from the point of view of reinforcement corrosion.

The use of HPC can also be recommended in regions that have a high concentration of chlorides, such as coastal regions, in structures such as buildings, bridges, and ports, the study of which is presented in the next section.

4.2.3 Case 3 – Regions with high chloride concentration - Maritime environment

Among the possible sources of chlorides mentioned in this study, the maritime environment deserves special attention due to its aggressive potential to reinforced concrete structures due to the high concentration of chloride ions in the environment.Poulsen and Mejlbro [4] propose a classification of different maritime exposure zones, being:

(i) maritime atmosphere zone: region located three meters or more above the maximum water level, including waves;

(ii) splash zone: region located between three meters above the maximum water level, including waves, and three meters below the minimum water level, including waves and

(iii) submerged zone: corresponds to the region located below three meters from the water level, including waves.

Therefore, the same concrete structure located in a maritime environment may have portions subjected to different exposure zones, in which there will certainly be different potential for chloride penetration, that is, different aggressive intensities.

Structures located in a maritime atmosphere zone present gradual contact with chlorides due to their concentration in the salt spray, which depends on variables such as wind, surface roughness, distance from the sea, and the capacity of the concrete surface to capture these ions. When relatively dry concrete is exposed to salt water, it can absorb it relatively quickly. Intermittent wetting and drying cycles, common in the splash zone, can successively accumulate high concentrations of chloride in concrete [46].

Studies by Wu, Li, and Yu [47] on the effects of exposure conditions on the diffusivity of chlorides in concrete indicated that the splash zone is the one that most severely affects the durability of reinforced concrete structures compared to the other areas of the maritime environment. Structures located in a splash zone are more prone to the transport of chlorides by capillary absorption in the surface layers and by diffusion within the concrete, where humidity levels remain higher.

In the case of structures in submerged areas, chloride transport occurs essentially by diffusion, a transport mechanism that occurs more slowly [48]. Furthermore, when concrete remains constantly submerged, chlorides penetrate to considerable depths, but there will be no corrosion unless there is oxygen present at the cathode [49].

One way to increase the useful life of structures exposed to maritime environments is the use of surface protectors on concrete. These can be classified into three groups: water repellents, pore blockers, and barrier or layer formers,

presented in a complementary manner in Appendix A.

The numerical approach adopted in this study for the maritime case does not take into account surface protections that use water repellents and pore blockers, as they involve the use of chemical agents or chemical reactions, respectively, and are not part of the scope of this study. On the other hand, the studies presented in Cases 1 and 2 may be related to the third type of surface protection, the so-called barrier or layer formed.

The formation of a barrier or layer is simulated in this study with thicknesses of 0.05 m and 0.025 m according to [50], using real values (not dimensionless as found in purely academic studies) for the physical and geometric parameters of the chloride diffusion problem, chloride diffusivity coefficients of the order of 10^{-11} and 10^{-12} (m^2/s), domain dimension in meters (m) and time interval of up to 31,536,000 seconds (1,000 years).

In Case 3, the numerical simulations were carried out with zero initial conditions for the concentration of chlorides in the problem domain (eq.(20)) and geometric and physical parameters similar to Case 2, presented in Table 2, however, using a higher concentration of chlorides in the external environment, twice as high as the value used in Cases 1 and 2, given by equation (22):

$$u(X_{\Gamma_1}, t) = 4 \qquad X_{\Gamma_1} \in \Gamma_1 \qquad (14)$$

which corresponds to a constant concentration of chlorides outside the coating layer along the entire contour and fixed for the entire analysis interval.

The results for Case 3 are presented below.

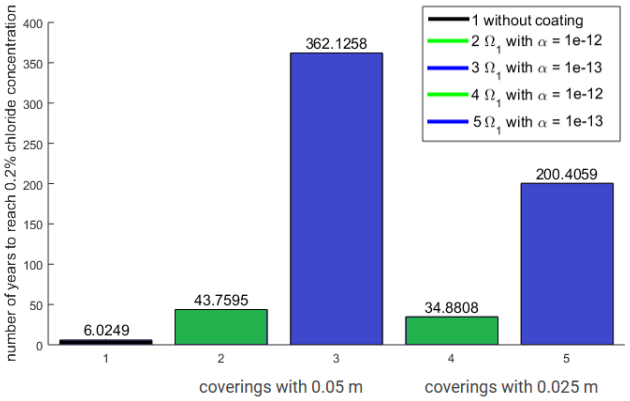

Fig. 12: Number of years to reach 0.2% of chloride concentration for different coating in a more aggressive environment. Uncoated (1), thickness of the coating layer = 0.05 m (2) and (3), 0.025 m (4) and (5).

Similar to the analysis applied in Case 2, Figure 12 presents the values referring to the number of years for the chloride concentration to reach 0.2% in the position of the steel rod R1 using the HPC in an environment with a higher concentration of chlorides. Comparing the results of Case 2 with those of Case 3 (Table 3), it is possible to observe in Case 3 the reduction in the number of years until the internal concentration of chlorides began to depassivate the steel. This is due to the higher concentration of chlorides in the external environment.

Calculating the percentage variation between the values obtained in Case 2 and Case 3, presented in the last line of Table 3, it is observed for Tests 2, 3, 4, and 5 using the barrier or coating layer, the average value of 0.34, indicating a reduction of approximately 34% in the number of years when the coated concrete structure is exposed to an environment that contains up to twice as many chloride ions.

Table 3: Comparison of the results of Cases 2 and 3 (years).

	Test 1	Test 2	Test 3	Test 4	Test 5
Case 2	13.3181	66.9077	549.5307	53.5895	298.7062
Case 3	6.0249	43.7595	362.1258	34.8808	200.4059
1- (Case 2/ Case 3)	0.547616	0.345972	0.341027	0.349111	0.329087

Table 3 also reveals very important information observed in the percentage value of Test 1 that does not use surface protection (barrier or coating layer), whose two-fold increase in the concentration of chlorides in the environment leads to a reduction of approximately 54% in the time required for the beginning of steel depassivation, even using high-performance concrete, significantly reducing the useful life of a reinforced concrete structure.

4.2.4 Analysis of results - General comments

The results obtained in Case 1 revealed that a coating layer composed of the concrete material itself is not efficient in preventing the depassivation of the steel, however, it can be stated that, with the application of each coating of 0.025 m thick with a coefficient of diffusivity coefficient equal to 1 x 10^{-13} m^2/s, the reinforcement will not suffer deterioration due to corrosion over 200 years, considering that the coating layer material does not change its permeability properties over time. Furthermore, if a 0.05 m layer of external coating with a diffusivity coefficient equal to 1 x 10^{-13} m^2/s is applied to the concrete, it can be stated that the reinforcement will not suffer deterioration due to corrosion during a period of at least 497 years, again assuming that the material maintains its permeability properties.

Still in Case 1, returning to Figures 7 and 9 (blue line), the effect of the coating layer on the diffusion process of chloride ions in reinforced concrete is evident, where it is possible to observe that the chloride concentration curves from the test 4, with 0.05 m and 0.025 m, show a very small inclination, almost horizontal, followed by a slightly higher rate, indicating that the chloride ions surpassed the coating layer and found a more permeable material, that is, concrete.

The results obtained in Case 2 revealed a significant increase in the time in which the reinforcement will not suffer

deterioration due to corrosion, demonstrating that HPC can increase the useful life of a reinforced concrete structure, especially when associated with an external coating layer with diffusivity coefficient with values in the order of magnitude of 10^{-12} or 10^{-13} m^2/s.

In Case 3, two important pieces of information were obtained from the simulation results. The first refers to the reduction in the number of years until the internal concentration of chlorides begins to depassivate the steel, around 34% less time, even using HPC associated with some coating layer. This reduction is due to the higher concentration of chlorides in the external environment, twice as high as in Case 2. The second further reinforces the need for studies on the use of a coating layer for reinforced concrete, given that the non-use of surface protection leads to a reduction of approximately 54% in the time required to begin steel depassivation, even using high-performance concrete, significantly reducing the useful life of a reinforced concrete structure.

The boundary conditions used in numerical simulations can be adapted to represent other sources of chlorides, as in the case of chloride-rich compounds added to water by urban sanitation companies, reaching reinforced concrete structures such as treatment tanks and/or reservoirs, or in the case of de-icing salts, used in regions where ice forms on roads and bridge decks, which, although necessary to provide safe winter driving conditions and save lives, can greatly contribute to the corrosion and degradation of construction structures.

Reinforced concrete structures require continuous maintenance to remain safe and in good working order and the study presented here, widely explored through computer simulations, shows that the execution of an external coating layer with a diffusivity coefficient of the order of 10^{-12} or 10^{-13} m^2/s when designed and executed early after the concrete has cured, can significantly extend the useful life of the reinforced concrete structure, as illustrated in Figures 8, 10, 11 and 12.

5. Conclusions

The D-BEM formulation presented in this article was developed and implemented to study the chloride diffusion equation in an isotropic medium. The computational codes were validated by comparing the numerical results of a problem in which the analytical solution was known, reaching a correlation level of 0.99954 for the R^2 estimator. Homogeneous subregions were used to simulate the section of a piece of reinforced concrete with external coating, simulating the application of an external coating layer representing surface protection for the concrete.

The results obtained with D-BEM demonstrated the effect of the migration of chlorine ions through the coating layer, as well as in the concrete itself, calculating the time necessary for the depassivation and the initiation of steel corrosion in reinforced concrete structures for different types of coating. The tests carried out, despite being presented in a simplified form and under specific limitations, presented at the end of section 2.1, simulate the phenomenon of chloride diffusion found in real cases in civil construction where reinforced concrete is used, given that the simulations considered the real values of the physical coefficients of the materials involved in the problem.

The chloride diffusivity coefficient of the order of 10^{-12} and 10^{-13} (m^2/s), used for the coating layer material, despite being thought of as composed of polymer material in the form of ink or epoxy, may be similar to high-performance concrete, being a material that is technically possible to be produced and executed as a mortar in layers of 0.05 m or 0.025 m thick, on the external part of the reinforced concrete structure.

Thus, after an extensive and in-depth analysis of the phenomenon of chloride diffusion in reinforced concrete, the results indicate that the proposed formulation, widely deduced and explored, serves as a simulation tool to test different types of concrete and materials used for the coating layer external, just by changing the geometry and the values of the coefficients, according to the dimensions of the reinforced concrete structure and the environment in which the structure will be inserted, presenting as a result, the time necessary until the beginning of the depassivation of the steel, the beginning of corrosion and the useful life of the structure.

It is understood that this type of study is frequently found in real applications in laboratories, using reinforced concrete samples and tanks with solutions rich in chlorides, however, the use of computer simulations appears as a non-destructive and very low-cost technique, with the possibility of simulating and testing the depassivation of reinforcement in very large concrete pieces, which would be impracticable to test in the laboratory.

Finally, to continue this study, it is suggested the use of other materials and thicknesses for the coating layer, the degradation of the coating layer itself, damage to the concrete, and its effects on the concentration of chlorides.

Conflict of Interest Statement

The authors declare that the research was conducted in the absence of any commercial or financial relationships that could be construed as a potential conflict of interest.

ACKNOWLEDGEMENTS

The author would like to thank UFPR and UFSC for their support inconducting this research.

References

[1] Bosc, Jean-Louis, et al. Joseph Monier et la naissance du ciment armé. Paris: Editions du Linteau, 2001.

[2] Alba, F. D. The First Patents for Reinforced Concrete.Changing Cultures.In: European Perspectives on the History of Portland Cement and Reinforced Concrete, Centuries, 2023.

[3] Tessari, R. Study of the protective capacity of some types of national cements, in relation to corrosion of reinforcement under the action of chloride ions. Master's Dissertation in Engineering – Federal University of Rio Grande do Sul, Porto Alegre, 2001.

[4] Poulsen, E.; Mejlbro, L. Diffusion of chloride in concrete: theory and application. Londres and Nova York: Taylor & Francis, pp 442, 2006.

[5] Andrade, C. Corrosion Processes in Hormigón and Modern Methods for Calculating Carbonation, Chlorine Penetration and Corrosion Propagation. In: LA CORROSIÓN MAJOR STUDIO COURSE, Actas, IETcc, Madrid, 2001.

[6] Cascudo, O. Contribution to the Study and Use of Electrochemical Techniques in Controlling Corrosion of Reinforced Concrete. São Paulo, 1991. Master's Dissertation in Civil Engineering – Polytechnic School, University of São Paulo, São Paulo, 1991.

[7] Silva, C. A.; Guimarães, A. T. V. C. Evaluation of the diffusion model considering the variation in time of the chloride content of the concrete surface. Revista Matéria, V. 19, N. 02, pp.81-93, 2014.

[8] Favretto, F.; Magalhães, F. C.;Guimarães, A. T. V. C.; Climent, M. A.; Real, M. V. Models for estimation of saturation degree of concrete through the environmental variables applied to the reliability analysis of reinforced concrete structures attacked by chloride ions. Revista Matéria, V. 26, N.03, 2021.

[9] Ferreira, P. R. R. Probabilistic modeling to predict the initiation time of chloride corrosion in reinforced concrete structures exposed in maritime atmosphere zones. Doctor's Thesis in Civil and Environmental Engineering - Technology Center of the Federal University of Paraiba, João Pesssoa, Paraiba, pp. 245, 2022.

[10] Tuutti, K. Service life of structures with regard to corrosion of embedded steel. In: Performance of concrete in maritime environment, ACI SP-65, 1980.

[11] Paiva, S. I. C. Study of the permeability of paints to chlorides. Internship report carried out at CIN - Northern Industrial Corporation, S. A., 2003.

[12] Brazilian Association of Technical Standards, ABNT - NBR 6118, Design of concrete structures – Procedure, Rio de Janeiro, Brazil, 2014

[13] Rocha, R. P. O.; Pettres, R. Digital reconstruction of a concrete pile from temperature data and boundary element formulation. Engineering Analysis with Boundary Elements, V. 153, pp. 267-294, 2023. DOI:10.1016/j.enganabound.2023.05.031

[14] Brebbia, C. A. The Boundary Element Method for Engineers. Pentech Press, London, 1978.

[15] Cheng, A.H.; Cheng, D.T. Heritage and early history of the boundary element method. Engineering Analysis with Boundary element, V. 29, pp. 268-302, 2005.

[16] Brebbia, C. A.; Dominguez, J. Boundary element An Introduction Course. Bath Press, Great Britain, 1989.

[17] Wrobel, L. C.; Brebbia, C. A. The dual reciprocity boundary element formulation for nonlinear diffusion problems. Computer Methods in Applied Mechanics and Engineering, V. 65, V. 2, pp. 147-164, 1987.

[18] Beer, G.; Watson, J. O. Introduction to Finite and Boundary Element Methods for Engineers. Wiley, England, 1994.

[19] Pettres, R. An introductory course on the boundary element method. V. 1, pp. 150 - 153, ISBN: 9798648732773, 2020.

[20] Yu, B.; Ning, C.; Li, B. Probabilistic durability assessment of concrete structures in maritime environments: Reliability and sensitivity analysis, China Ocean Engineering, V.31, pp.63-73, 2017.

[21] Guimarães, A.T.C.; Helene, P.R.L. Models for Predicting Service Life in the Maritime Environment. In: 42nd Brazilian Concrete Congress - IBRACON, Fortaleza, Ceara, Brazil, 2000.

[22] Climent, M.A.; Vera, G.; López, J.F.; et al. A Test Method for Measuring Chloride Diffusion Coefficients Through Nonsaturated Concrete Part I: The Instantaneous Plane Source Diffusion Case, Cement and concrete Research, V. 32, pp. 1113-1123, 2002.

[23] Nielsen, E.P.; Geiker, M.R. Chloride diffusion in partially satured cementitions material, Cement and Concrete Research, V. 33, pp. 133-138, 2003.

[24] Guimarães, A.T.C. Transport of chloride ions in concrete: influence of the degree of saturation. In: PATORREB: 3rd Meeting on Pathology and rehabilitation of buildings/3rd Congress of Pathology and Rehabilitation of Buildings, Porto, Portugal, 2009.

[25] Martys, N.S.Diffusion in partially-saturated porous materials. Materials and Structures, V. 32, pp. 555-562, 1999.

[26] Mercado-Mendoza, H.; Lorente, S.; Bourbon, X.The Diffusion Coefficient of Ionic Species Through Unsaturated Materials, Transport in Porous Media, V. 96, Issue 3, pp. 469-481,2012.

[27] Mercado-Mendoza, H.; Lorente, S.; Bourbon, X. Ionic aqueous diffusion through unsat rated cementitious materials – A comparative study, Construction and Building Materials, V. 51, pp. 1-8, 2014.

[28] Magalhães, T. A. Analysis of the penetration of chloride ions in cementitious composites containing different levels of blast furnace slag. Master's Dissertation in Engineering – Federal University of Minas Gerais, School of Engineering, 2019

[29] Helene, P. R. L. Contribution to the study of corrosion in reinforced concrete reinforcement. Doctoral thesis. Polytechnic School of the University of São Paulo, São Paulo, 1993.

[30] Reis, L. S. N. About the recovery and reinforcement of reinforced concrete structures. Masters dissertation. Postgraduate Program in Structural Engineering at the Federal University of Minas Gerais. Belo Horizonte, MG, Brazil, 2001.

[31] Oliveira, J. R. S.; Pettres, R. A thermal analysis of concrete structures performed by layers using boundary element formulation and dual reciprocity, Eng Analysis with Boundary Elements, V.150, pp. 542-554, 2023. https://doi.org/10.1016/j.enganabound.2023.02.023

[32] Pettres, R. A first dynamic population invasion study from reactive-telegraph equation and boundary element formulation. Eng. Anal. Bound. Elem. V. 122, pp. 214–31, 2021. https://doi.org/10.1016/j.enganabound.2020.11.002.

[33] Pettres, R.; Lacerda, L. A.; Carrer, J.A.M. A boundary element formulation for the heat equation with dissipative and heat generation terms. Eng Anal Bound Elem; V. 51, pp. 191–198, 2015. https://doi:10.1016/j.enganabound.2014.11.005.

[34] Montgomery, D. C.; Runger, G. C. Applied Statistics and Probability for Engineers. Student Workbook with Solutions, 3rd Edition. USA: WILEY, 2003.

[35] Pettres, R.; Cirilo, E. R. A first advective velocity study in porous media using temperature measures and boundary element formulation. Eng Anal Bound Elem; V. 121, pp. 217–32, 2020. https://doi.org/10.1016/j.enganabound.2020.10.001.

[36] Pettres, R.; Pettres, A. A.; Cirilo, E. R. A second dynamic population invasion study from reactive telegraph equation and boundary element formulation – a numerical assay about tumour growth in vitro, Journal of Biotechnology and Biodiversity, V. 10, N. 2, 2022. https://doi.org/10.20873/jbb.uft.cemaf.v10n2.pettres

[37] Boletin 152. Durability of concrete structure. Comitê Euro-Internacioal Du Béton. In: CEB 152 - EUROPE, 1992.

[38] Arora, P. et al. Corrosion initiation time of steel reinforcement in a chloride environment—a one dimensional solution. Corrosion Science, Elsevier, V. 39, N. 4, pp. 739–759, 1997.

[39] Lin, S. Chloride diffusion in a porous concrete slab. Corrosion, V. 46, N. 12, pp. 964–967, 1990.

[40] Page, C. L.; Short, N. R.; El Tarras, A. Diffusion of chloride ions in hardened cement paste. Cement and Concrete Research, N. 11, pp. 395-406, 1981.

[41] Malier, Y. High Performance Concrete: From material to structure, 1st ed., CRC Press, 1992. https://doi.org/10.1201/9780203752005

[42] Mehta, P. K.; Monteiro, P. J. M. Concrete Microstructure, Properties, and Materials – Fourth Edition. Ed.: McGraw Hill. ISBN.: 978-0-07-179787-0. pp.675, 2013.

[43] Wood, J. G. M.; Wilson, J. R.; Leek, D. S. Improved Testing of Chloride Ingress Resistance of Concretes and Relation of Results to Calculated Behavior, In: Proceedings of the Third International Conference on Deterioration and Repair of Reinforced Concrete in the Arabian Gulf, Bahrain Society of Engineers and CIRIA, 1989.

[44] Cascudo, O.Corrosion control of concrete reinforcement – inspection and electrochemical techniques. Goiânia, GO: Editora UFG, pp. 237, 1997.

[45] Cascudo, O. Inspection and Diagnosis of concrete structure with reinforcement corrosion problems, Concrete: Teaching, Research and Achievements, IBRACON, V. 2, pp.1071 – 1108, ed. Geraldo C. Isaia, São Paulo. 2005.

[46] Gjorv, O. E. Durability design of concrete structures in severe environments. Second edition, Boca Raton: CRC Press, pp. 254, 2014.

[47] Wu, L.; Li, W.; Yu, X. Time-dependent chloride penetration in concrete in maritime environments. Construction and Building Materials, V. 152, pp. 406-413, 2017.

[48] Meira, G. R. Corrosion of reinforcement in concrete structures: Fundamentals, diagnosis and prevention. João Pessoa,pp. 127, Ed. IFPB, 2017.

[49] Neville, A. M. Concrete properties. Fifth edition. São Paulo, PINI, pp. 912, 2015.

[50] Medeiros, M. H. F.; Real, L. V.; Quarcioni, V. A.; Helene, P. Concrete with surface protection and exposed to chloride solution: Equivalent covering thickness. ALCONPAT Magazine, V. 5, N. 3, pp. 219 – 233, 2015

[51] Medeiros, M.; Helene, P. Efficacy of Surface Hydrophobic Agents in Reducing Water and Chloride Ion Penetration in Concrete. Materials and Structures, V. 41, N. 1, pp. 59-71, 2008.

[52] Medeiros, M. H. F.; Helene, P. Durability and protection of reinforced concrete, Techne, V. 151, pp. 50-54, 2009.

[53] Jacob, T.; Hermann, K. Protection of concrete surfaces: hydrophobic impregnations, Construcción y Tecnología, pp. 18-23, 1998.

[54] Batista, M. Siloxane and silane - perfects hydrophobics agents for all situations, Recuperar Magazine, V. 23, pp. 14-19, 1998.

[55] Mariconi, G.; Tittarelli, F.; Corinaldesi, V. Review of silicone-based hydrophobic treatment and admixtures for concrete, Indian Concrete Journal, V. 76, N. 10, pp. 637-642, 2002.

[56] Brough, A. R.; Atkinson, A. Sodium silicate-based, alkali-activated slag mortars - Part I. Strength, hydration and microstructure, Cement and Concrete Research, V. 32, pp. 865–879, 2002.

[57] Jones, J. W. Method of Hardening and Polishing concrete floors, walls, and the Like, United States Patents. Patent number: US 6,454,632 B1. Sep. 24, 2002.

[58] Toledo Filho, R. D.; Ghavami, K.; George, L. England and Karen Scrivener Development of vegeeq fiber–mortar composites of improved durability, Cement and Concrete Composites, V. 25, N. 2, pp. 185-196, 2003.

[59] Thompson, J. L.; Silsbee, M. R., Gill, P. M., Scheetz, B. E. Characterization of silicate sealers on concrete, Cement and Concrete Research, V. 27, N. 10, pp. 1561-1567, 1997.

[60] Medeiros, M. H. F.; Pereira, E.; Figura, A. S.; Tissot, F. M.; Artioli, K. A. Evaluation of the efficiency of surface protection systems for concrete: water absorption, chloride migration and contact angle, Materia - UFRJ, V. 20, pp. 145-159, 2015.

[61] Delucchi, M.; Barbucci, A.; Cerisola, G. Crack-bridging ability and liquid water permeability of protective coatings for concrete, Progress in Organic Coatings, V. 33, pp. 76-82, 1998.

[62] Seneviratne, A. M.; Sergi, G.; Page, C. L. Performance characteristics of surface coatings applied to concrete for control of reinforcement corrosion, Construction and Building Materials, V. 14, pp. 55-59, 2000.

[63] Uemoto, K. L.; Agopyan, V.; Vittorino, F. Concrete protection using acrylic latex paint: Effect of the pigment volume content on water permeability, Materials Structures, V. 34, pp. 172-177, 2001.

[64] Al-Zahrani, M. M.; Al-Dulaijan, S. U.; Ibrahim, M.; Saricimen, H.; Sharif, F. M.Effect of waterproofing coatings on steel reinforcement corrosion and physical properties of concrete, Cement and Concrete Composites, V. 24, pp. 127-137, 2002.

Appendix

A.1 Water-repellents

Water-repellent agents are chemicals designed to repel water and protect porous surfaces, such as concrete, from water penetration and moisture absorption. Water-repellents work mainly by filling the pores on the concrete surface and reducing its ability to absorb water. Currently, the most used materials are silanes, oligomeric siloxanes and a mixture of these two compounds [51]. Chemically, silanes are formed by small molecules that contain a silicon atom and siloxanes are small chains of a few silicon atoms, whose molecules contain alkoxy (organic) groups linked to the silicon atom. The silanes and siloxanes react with the silicates in the concrete, forming a stable adhesion. Medeiros and Helene [52] showed that the penetration of water-repellent agents is better on the abrasion faces than on those in contact with the formwork, due to the greater permeability of the former. Jacob and Hermann [53], Batista [54] and Moriconi et al. [55] presented a broad literature review on water-repellent agents. The use of these agents in the construction industry is growing at an interesting rate and has been reasonably studied. However, there are some items still under study, such as the influence of the water penetration mechanism (capillarity suction and permeability) on the effectiveness of treatment with water-repellents [51].

A.2 Pore blockers

Pore blockers such as sodium silicate play an important role in the cement industry, it is used for several other specific purposes in the production of cement and related products. For example: as a slag cement activator, as a protective additive for plant fibers in cement composites, as a surface hardener for industrial floors and as a surface protection system for concrete [42, 56, 57, 58].

The lack of published technical and scientific information about these products can be a challenge. On the other hand, there are various products sold and recommended for protecting the concrete surface. The choice of protection method will depend on the specific needs of the project and the environmental conditions in which the concrete will be exposed. Thompson et al. [59] explained the three theories of how silicates act to improve the performance of concrete:

(i) Precipitation of SiO_2 in pores;
(ii) Formation of an expansive gel, similar to that formed in the alkali silicate relationship, within the pores;
(iii) Reaction of silicates with calcium hydroxide present in the pores, forming hydrated calcium silicate.

According to Medeiroset al. [60], the last theory is the most accepted currently. Therefore, theoretically, pore blockers are products composed of silicates, which penetrate the surface pores and react with portlandite to form C-S-H, generating a less porous layer in the surface layer of the concrete.

A.3 Barrier or layer formers

Barrier former or layer former are effective in covering cracks up to 0.1mm in the concrete surface. However, if the concrete cracks after application, the layer may break at these points, leaving the underlying concrete exposed to the external environment. This type of surface treatment (barrier former) was studied by Delucchi et al. [61], who indicated the importance of the *E* parameters (viscosity modulus) in barrier adhesion. Seneviratne et al. [62], basing their studies on elasticity and thermomechanical analysis, suggested that the most successful barrier is one with the ability to maintain its elastomeric properties throughout the necessary period of exposure and over a wide range of operating temperatures. Uemoto et al. [63] showed the correlation between the volumetric content of the paint pigment and its water permeability. Al-Zahrani et al. [64] showed that protection systems based on barrier formers present accelerated corrosion inhibition efficiency consistent with the results obtained in physical properties, in particular, water absorption, permeability and penetration of chloride ions. Medeiros and Helene [52] state that the determination of the chloride diffusion coefficient allows a quantitative comparison of protection systems and, therefore, its calculation must be made possible in migration tests. Barrier formers are probably the most used in the construction industry, and this may be the reason they are extensively studied in comparison with other surface protection systems.